BULLETIN OF THE POLISH ACADEMY OF SCIENCES
TECHNICAL SCIENCES, Vol. 74(6), 2026, Article number: 2513
DOI: 10.24425/bpasts.2026.2513

Artificial neural network-based detection of fluids and scale in petroleum pipelines via capacitive and electromagnetic sensors

Hala H. ALHASHIM*

Department of Physics, College of Science, Imam Abdulrahman Bin Faisal University, Dammam, 31441, Saudi Arabia

Abstract. Accurate measurement of volume fractions (VF) in multiphase flows is often challenged by the presence of scale layer deposits on the internal pipe walls. This study presents a robust, non-invasive intelligent metering system designed for simultaneous estimation of scale thickness and VFs of oil, water and gas phases. The methodology integrates data from two distinct sensing modalities: a twin rectangular fork-like capacitive sensor, simulated using COMSOL Multiphysics, and gamma-ray attenuation (Co-60 source), calculated via the Beer-Lambert law. To process this hybrid dataset, various multilayer perceptron (MLP) neural network architectures were developed and optimized in MATLAB. The proposed model achieves high precision, predicting the VFs of gas, water and oil with mean absolute errors (MAE) of 0.027, 0.032, and 0.033, respectively. Furthermore, the scale layer thickness was estimated with a remarkable MAE of 0.244 mm. These numerical results confirm the efficiency of the proposed sensor fusion technique in mitigating the adverse effects of scale on measurement accuracy, offering significant advancement for real-time monitoring in the petroleum industry.

Keywords: three-phase flow; volume fractions; scale layer thickness; artificial neural network; capacitive sensor; gamma-ray sensor.

1. INTRODUCTION

Flow measurement is very important in many industries. One key task is measuring volume fraction (VF) in multiphase flows like oil, water and gas pipelines [1]. Flow measurement methods are generally divided into two types: traditional and non-invasive. Traditional tools such as sampling tubes, vibrating densitometers and turbine meters, have complex structures and slow response, and often require stopping or separating the flow, which reduces efficiency [2]. Non-invasive methods solve many of these problems. They work without direct contact or separating materials inside the pipe and can operate in different environments. Examples include capacitance sensors and gamma-ray attenuation sensors [3]. Capacitance-based sensors are widely used in multiphase flow measurement, especially in oil and gas industries where flow monitoring is complex [4]. For example, electrical capacitance volume tomography (ECVT) was used in subsea pipelines to measure mass flow rate, velocity and volume fraction of oil, gas and water [5]. A planar array sensor was introduced for fast imaging of multiphase flow and surface-mounted use [6]. Gamma-ray methods have also been studied for non-destructive oil-water flow measurement and optimization [7]. Recently, artificial neural networks (ANN), machine learning and deep learning have become important for analyzing sensor data [8]. ANNs were used to predict void fraction in air-water flow using capacitance sensor data [9]. Other studies used capacitive sensors, photon attenuation sensors and MLP networks to measure gas-oil-water proportions with good accuracy [3, 10, 11]. Scale buildup in oil and gas pipelines is a major problem because it reduces measurement accuracy. Researchers have used gamma-ray absorption, pressure sensors, capacitance and impedance methods to monitor flow and scale [12]. Ultrasonic flow meters, electrical capacitance tomography (ECT) and laser profilometry are also used to measure scale thickness [13]. Gamma radiation is effective because it penetrates pipe walls and measures density and scale thickness accurately, even under high-pressure conditions [14]. Combining gamma-ray techniques with AI has improved scale prediction and measurement accuracy [15–19]. In this paper, a new metering system is proposed. It combines a photon attenuation sensor, a capacitance sensor and an AI-based model. The system predicts oil-water-gas volume fractions and scale thickness at the same time. The method achieves high accuracy with low MAE. The novelty of the proposed measurement technique lies in its capability for simultaneous determination of volume fractions (VFs) and scale thickness. This issue is particularly important in the industries where three-phase mixtures (gas, water and oil) are common, such as offshore oil and gas production. In these environments, the phase composition changes continuously due to flow fluctuations and varying oil-to-water ratios. These dynamics lead to significant measurement errors when using conventional capacitance-based or conductivity-dependent methods. Therefore, developing a composition-independent measurement technique directly contributes to improving flow monitoring accuracy and operational safety in these applications. Although previous studies have primarily reported measurement methods and ANN-assisted estimation models that focus on either

*e-mail: Halhashim@iau.edu.sa

Manuscript submitted 2026-04-30, revised 2026-07-04, initially accepted for publication 2026-07-07, published in November 2026.

© 2026 The Author(s). This is an open access article under the CC BY license (http://creativecommons.org/licenses/by/4.0/)

volume fractions or scale thickness independently, a significant gap remains in the simultaneous characterization of these parameters. The present study addresses this limitation by proposing a measurement approach capable of concurrent estimation of all volume fractions and scale thickness. Using single non-invasive sensors integrated with an optimized ANN model, this work provides a more comprehensive monitoring solution for complex industrial multiphase flows. The next sections describe the sensors, ANN models and settings, results and then conclusions. The novelty of this work is not based on the use of COMSOL simulations, since simulation-assisted sensor development is already well established in the literature. Rather, the contribution lies in the proposed measurement strategy, which combines an optimized capacitance sensor, a properly selected Co-60 gamma-ray source, and an ANN framework to simultaneously estimate three phase volume fractions and scale thickness using a minimal hardware configuration.

2. EMPLOYING TWO DISTINCT SENSORS TO GENERATE DATA FOR THE NETWORK

The main focus of this investigation is measuring VFs of an oil-water-gas mixed fluid along with the scale thickness inside the pipeline. To achieve this goal, an MLP ANN will be utilized. This model needs inputs to measure the desired parameters. Hence, appropriate sensor(s) must be used to generate enough data for it. The chosen sensor has to be non-destructive because another aim of this study is measuring parameters without interrupting the process or separating phases. To opt for selecting the best sensor, the ones that are suitable for measuring volume fractions of multiphase fluids must be selected. Among all existing sensors, two types of them are widely-used in the abovementioned subject, capacitance-based and gamma-ray attenuation sensors. This is because of their high level of accuracy, accessibility and installation being not complex. Since the investigated fluid is a multiphase type, based on [3], just using one of these sensors cannot measure all volume fractions. Hence, both of them are utilized with the aim of measuring volume fractions along with the thickness of scale. This approach can be found in the literature but the main novelty of this paper is measuring VFs of all phases and scale thickness, simultaneously and accurately. Therefore, the twin rectangular fork-like capacitance (TRFLC) sensor presented in [20] and a photon attenuation sensor with Co-60 in its source side are utilized to reach the goals of this study. Capacitance-based sensors operate by measuring changes in capacitance, which occurs when the material between two electrodes (known as the dielectric) changes. In applications such as pipeline monitoring, the dielectric is the material being present inside the pipe. Changes in the material, for instance, in its relative permittivity, will affect the sensor's capacitance. This means that the dielectric characteristics of the materials inside the pipe highly affect the capacitive sensors, with the most prominent impact coming from changes in relative permittivity. Capacitance sensors offer several advantages, such as low cost, simple design, fast response and non-invasive installation. The relationship between the sensor's capacitance (C) and the dielectric properties of the material is described in (1) where ε_r is the relative permittivity, ε_0, being around 8.854×10^{-12} F/m, is the free space permittivity, A is the area of overlap between the electrodes, and D is the distance between them [6]. This equation shows that capacitance is directly proportional to the relative permittivity of the material, highlighting the sensor's sensitivity to changes in the dielectric characteristics of the fluid.

$$c = \frac{\varepsilon_r \varepsilon_0 A}{D}. \tag{1}$$

To generate data for the modeled network, the TRFLC sensor is simulated in widely-used software. TRFLC geometry is selected because it has better sensitivity in comparison with other types of capacitance-based sensors, such as concave and ring ones. One of key steps before generating data is validating the software that the sensor is supposed to be simulated in and its environment. There are a number of published papers that have investigated the validity of data generated by COMSOL Multiphysics software [9]. In these studies, experimental-oriented investigations have been performed by means of making static models and comparing experimental results with those of the aforementioned software. According to their findings, there were close trends between simulated and manufactured models' outputs, proving the software validity. Hence, in this paper, COMSOL Multiphysics software is utilized with the aim of designing and simulating the TRFLC sensor being a capacitance-based sensor. The created sensor and its components, ranging from pipe to fluid, are illustrated in Fig. 1a. The pipe's thickness, the fluid's radius and the pipe's interior radius are shown as T1, R1, and R2 in Fig. 1b, respectively. While the pipe's thickness is equal to 0.6 cm, the radius of fluid and scale thickness are completely dependent on each other. For instance, when there is a 0.3 cm of scale, the fluid's radius is equal to 2.3 cm because the pipe's interior radius is equal to 2.6 cm. Since the considered range to investigate scale thickness is from 0 cm to 1 cm, various states of scale thickness, with step of 0.1 cm are considered. Side and back view of the simulated sensor are presented in Fig. 1c and Fig. 1d, respectively. In these figures, the length of the pipe (L1) is equal to 18 cm. Moreover, L2, L3 and G1 are equal to 10.5 cm, 1 cm and 0.5 cm, correspondingly. This means the length of each electrode is equal to 12 cm.

To evaluate data obtained from the software, an experimental setup was made. This way, the performance of the sensor used in the real world can be evaluated, too. To implement a water-gas homogeneous fluid in the setup prepared, several yellow straws, made from plastic with a thickness of 0.5 mm, were placed inside a glass pipe with a radius of 3.2 cm. The length of this pipe was 20 cm. Also, the geometry of the sensor was applied on the surface of the pipe with a copper plate whose thickness was 0.6 cm. All measurements were done by an LCR meter (its model: GPS-3135C), which can measure capacities from 0.00001 pF and 9999.99 mF. The frequency range of this device is from 50 Hz to 100 kHz with testing signal revolution equal to 10 mV. The settings on the LCR meter were fixed at 2 volts for the voltage and 200 kHz for the frequency. The trends of both simulated and prepared sensors were highly close

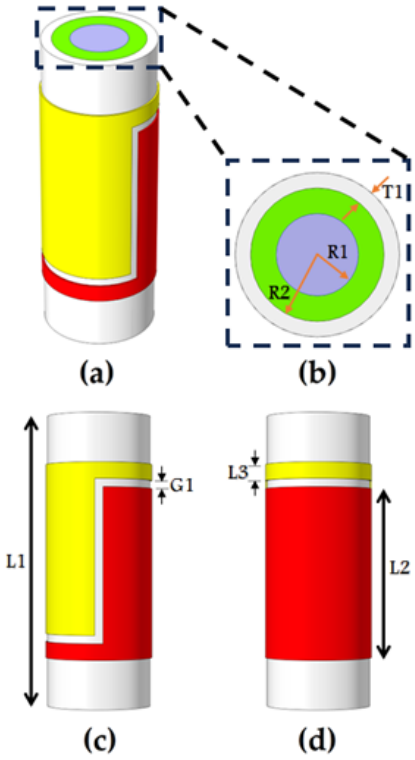

Fig. 1. Designed TRFLC sensor, (a) 3D view, (b) different radiuses, (c) sensor's side view, and (d) sensor's back view

together, and this shows that the simulated results can be used as valid datasets. Moreover, to make sure the results were consistent regardless of where the materials were placed inside the sensor (to check the spatial distribution), the tests were repeated several times. Then the position of the full straws for each volume fraction was changed. The results from these repeated tests showed only a small difference, confirming the consistency of the measurements. The experimental setup is illustrated in Fig. 2. The mean relative difference between the normalized experimental and simulated data is 1.634%, with maximum deviation of less than 3% across all void fractions. This minimal discrepancy clearly demonstrates that the simulated and experimental data are in excellent agreement, thereby validating reliability of the



Fig. 2. Measuring different volume fractions of the experimental sensor prepared

simulated geometry. Consequently, the simulation model has been successfully verified and can be confidently utilized for generating new data.

Because relative permittivity of materials such as gas and oil is so similar, capacitance sensors struggle to accurately measure all phases' VF in a multi-phase mixture. To address this, utilizing additional sensors, such as a density-based photon attenuation sensor, can be the solution. Gamma-ray sensors are effective tools for measuring the density of materials, and have been used since the 1950s to measure volume fractions in multi-phase mixtures. These sensors work by detecting how much gamma radiation is absorbed or "attenuated" as the rays pass through a liquid. In a typical setup, a gamma ray is emitted from a source, travels across the pipe and reaches a detector on the other side. The intensity of the gamma rays is measured at two points: initially, as the rays leave the source (Ix), and after they pass through the pipe and fluid to reach the detector (Iy). The sensor generates its output by analyzing the variation between the two intensity levels, allowing it to infer the material's density flowing through the pipe. This method is non-destructive, and its sensitivity to density makes it a reliable option for monitoring various phases in the studied mixture. In Fig. 3, positioning of the sensor and the pipe as well as their various components are illustrated. As it is clear, parts 4, 5 and 6 are pipe, homogeneous fluid and scale, respectively. While part 2 shows the source (Co-60) of the sensor, part 7 depicts its detector. There are two collimators and shields for both source and detector sides presented as part 1 and 3, correspondingly.

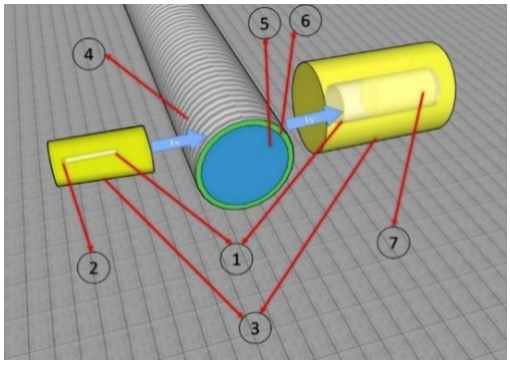

Fig. 3. Positioning of gamma-ray attenuation sensor beside the pipe

The Beer-Lambert law explains how the density of a material affects the operation of a photon attenuation sensor. Based on it, presented by (2), the intensity of the gamma rays, passing through a material, decreases depending on the material's density and thickness. The energy of the ray emitted from the source is represented by Ix, while Iy is the energy received by the detector. The absorption coefficient (η), the density (ρ) of the material, and the thickness of the material (L) all influence this attenuation. By incorporating linear attenuation coefficients (μ) presented in [21], Iy/Ix intensities can be calculated, which provides a measure of how much radiation is absorbed by the material. VFs of each phase, denoted as α, β and γ for gas, water and oil, respectively, are used to calculate the final result. This

equation allows gamma-ray sensors to determine the density and composition of multi-phase fluids in pipelines. This way, the second input for the modeled network is provided.

$$\ln\left(\frac{I_y}{I_x}\right) = -\left[\alpha\mu(E)_{\text{oil}} + \beta\mu(E)_{\text{water}} + \gamma\mu(E)_{\text{gas}}\right] \times L. \quad (2)$$

This study uses Cobalt-60, a gamma-ray source with high penetration power and a long half-life, emitting radiation at two energies: 1.17 MeV and 1.33 MeV, which are well-suited for penetrating materials in pipelines. For the scale measurement, the material BaSO4 (with relative permittivity of 11.4 and density of 4.48 g/cm^3) is used. Moreover, relative permittivity of gas is 1, relative permittivity of water is 81, and relative permittivity of oil is 2.2. Also, density of gas, water and oil is 0.001 g/cm^3, 1 g/cm^3 and 0.9 g/cm^3, respectively [3]. The focus is measuring all three volume fractions along with scale thickness of a three-phase flow where the proportions of each phase are varied from 0% to 100%, with 10% intervals, and the scale thickness is varied from 0 cm to 1 cm, in 0.1 cm intervals.

3. UTILIZING AN MLP ANN WITH THE AIM OF PREDICTING PARAMETERS

ANNs are extensively applied in various domains, including signal processing and pattern recognition, because they can model complex relationships between variables. In this research, ANNs are used because they are highly effective at handling nonlinear relationships, which are common in multiphase flows measurements. Multiphase systems are inherently dynamic in nature, and the measurements obtained from capacitance and gamma-ray sensors frequently demonstrate complex, nonlinear relationships as well as strong interdependencies between variables, making their analysis and interpretation more challenging. ANNs can learn these complex patterns from data, making them useful for understanding these types of systems. Among different types of ANNs, the multi-layer perceptron (MLP) is especially popular for volume and scale measurements due to its flexibility and ability to handle nonlinear functions [22]. MLPs can approximate continuous functions well, making them suitable for unpredictable systems. Unlike other models such as Gaussian process regression (GPR), which can be slow with large datasets, MLPs can take advantage of powerful hardware like GPUs, speeding up the training process [23]. In this study, to measure volume fractions along with the scale layer's thickness inside a channel conveying a mixed fluid, an MLP ANN is employed. The MLP network consists of various layers containing input, hidden and output layers, with neurons in each layer using activation functions like sigmoid, tansig or the linear ones. During training, the network adjusts its weights and biases to minimize the error. The learning rate, which controls how quickly the network adjusts, is set to 0.01 after testing different values. The Levenberg-Marquardt (LM) algorithm [24] and [25], known for combining Gauss-Newton and gradient descent methods, is used to optimize the network and speed up convergence. This makes it a good choice for complex problems like multiphase flow measurement. After gathering data from the simulated sensor in COMSOL Multiphysics software and the calculated gamma rays by using Beer-Lambert equations, they were normalized before transferring to MLP ANN. The network's performance was optimized by adjusting hyperparameters like the number of hidden layers, activation functions, neurons in each layer, and so on. Eventually, the proposed network possessing the lowest error was selected for this study. The finalized network architecture incorporated two input features: one derived from capacitance measurements obtained through COMSOL simulations, and the other based on Beer-Lambert law calculations using Cobalt-60 gamma radiation. The proportions of each phase (gas, water and oil) varied from 0% to 100%, in 10% increments, and the scale thickness ranged from 0 cm to 1 cm, with 0.1 cm steps. This resulted in a total of 726 calculations and simulations. The dataset was randomly partitioned, allocating 70% (520 samples) for training purposes, while the remaining 30% (206 samples) were reserved for testing. The network consisted of two hidden layers, with 18 neurons in the first layer and 16 neurons in the second. The hidden layers employed the tansig activation function, as defined in (3), whereas the input and output layers utilized the purelin activation function, described in (4). The tansig activation function was used in the hidden layers to capture nonlinear relationships, while the purelin function in the output layer allows for continuous output variation, which is appropriate for regression-based estimation of void fraction. The network had four outputs and was trained for 3000 epochs to minimize MAE.

$$\text{Tansig}(n) = \frac{2}{1+e^{-2n}} - 1, \quad (3)$$

$$\text{Purelin}(n) = n. \quad (4)$$

In this part, the network's outputs regarding train and test sets of all four outputs, volume fractions of gas, water and oil along with scale thickness are presented. As mentioned before, measuring all three volume fractions and the scale layer's thickness are the main goals of this study. To fulfil this mission, the TRFLC sensor was simulated in COMSOL software and gamma rays were calculated by related equations to generate two distinct groups of data. By these inputs, models were trained and tested with various hyperparameters for a number of times to reach the best network. The best MLP ANN had the training set's MAE equal to 0.112, 0.026, 0.024 and 0.022 for scale thickness, VF of gas, VF of water and VF of oil, respectively. With the same order, the network achieved the testing set's MAE equal to 0.244, 0.027, 0.32 and 0.033. As it is clear, all four outcomes note very low amount of error for both their train and test data sets. This highlights the ability of this approach to estimate VFs of a gas-water-oil blended flow along with measuring the thickness of scale inside the pipe, accurately. Moreover, the proposed network has predicted all outputs without getting involved with overfitting or underfitting. As mentioned before, the first step was designing and simulating the TRFLC sensor in the validated software, COMSOL. Simultaneously, the Co-60s detected were counted by means of Beer-Lambert equations. Both data groups were generated in this manner. In the following, both groups were accumulated and then normalized. The latter step was for

putting all data in a constant range, for example, from 0 to 1. The next step was followed by dividing data between train and test sets, randomly. After checking a number of networks with different hyperparameters, the best network was selected, possessing very low MAE for all four outputs. Finally, all outputs were displayed. Regarding the ANN details, a total dataset of 726 samples was generated by changing the gas, water and oil volume fractions from 0% to 100% in 10% steps, and the scale thickness from 0 cm to 1 cm in 0.1 cm steps. Before training, all data obtained from the COMSOL simulations and the Beer-Lambert equations were normalized between 0 and 1 to ensure consistent learning. A multi-layer perceptron network was used, consisting of an input layer with 2 features (capacitance data and gamma-ray intensity), two hidden layers with 18 neurons in the first layer and 16 neurons in the second layer, and an output layer with 4 nodes to predict all targets simultaneously (scale thickness, gas's VF, water's VF and oil's VF). The tansig activation function was used for the hidden layers, and the purelin function was applied to the output layer. The tansig activation function was used in the hidden layers to capture nonlinear relationships, while the purelin function in the output layer allows for continuous output variation, which is appropriate for regression-based estimation of void fraction. The network was trained for 3000 epochs using the Levenberg-Marquardt optimization algorithm with a learning rate of 0.01 for fast convergence. To prevent overfitting, the dataset was randomly split into 70% (520 samples) for training and 30% (206 samples) for testing, and the training error was closely tracked by the testing error, which proves good generalization. Finally, the model's accuracy was evaluated using three standard metrics: mean absolute error, mean squared error and root mean squared error, which are detailed in Section 3.1 and shown in Fig. 4. The equilibrium between training and testing errors demonstrates that the network generalizes effectively to unseen data and is not affected by underfitting.

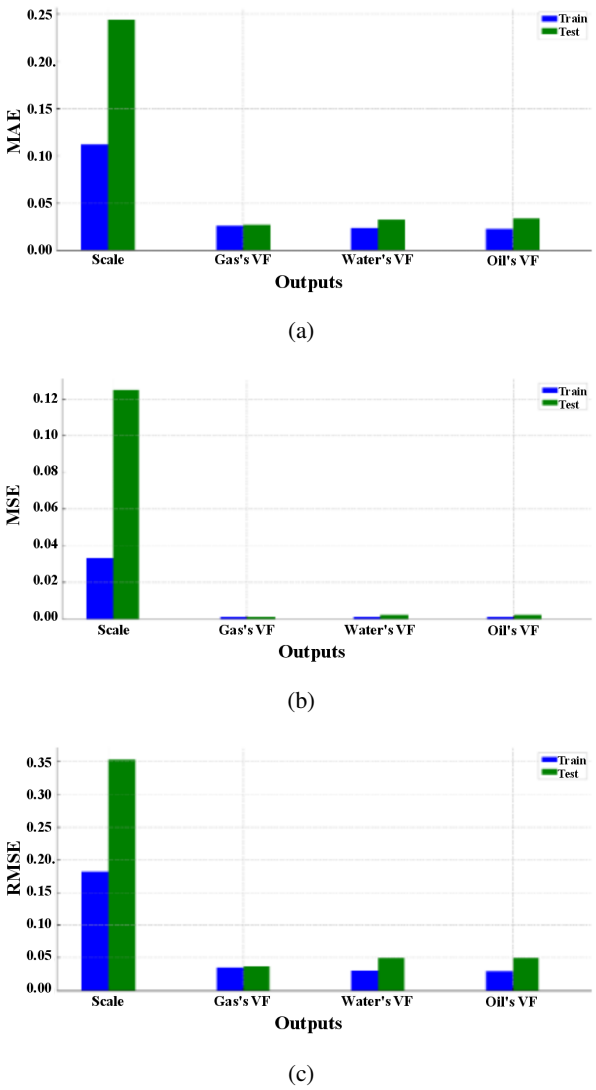

Fig. 4. Obtained outputs' error, (a) MAE, (b) MSE, and (c) RMSE

3.1. Error analysis

In Fig. 4, the performance of the network is evaluated using three widely used error metrics: MAE by formula (5), mean squared error (MSE) by formula (6) and root mean squared error (RMSE) by formula (7). MAE provides a straightforward measure of average prediction accuracy, reflecting the magnitude of error without giving excessive weight to outliers. In contrast, MSE amplifies the influence of larger prediction errors, which makes it more sensitive to outliers and which can highlight larger deviations in the model's performance. RMSE, being the square root of MSE, provides a metric with the same units as the data, making it more interpretable in real-world contexts. As can be seen in Fig. 4a, the proposed approach measured volume fractions of gas, water and oil with an MAE equal to 0.027, 0.032 and 0.033, respectively. With the same order, their MSE in Fig. 4b are equal to 0.0013, 0.0024, and 0.0024, which by calculating the roots of them, RMSE, illustrated in Fig. 4c, can be calculated at 0.036, 0.049, and 0.049. Aside from reaching very low error for measured volume fractions, the presented metering system was completely successful in predicting the scale thickness, simultaneously. MAE, MSE and RMSE of scale thickness outputs are equal to 0.24, 0.125 and 0.353, correspondingly. These results are very low, too. All of these errors, obtained from running the proposed network, prove the novelty of the presented metering system that can to measure volume fractions of a fluid containing gas, oil and water along with estimating the scale layer's thickness.

$$\mathrm{MAE} = \frac{1}{n}\sum_{i=1}^{n}\left|X_i - Y_i\right|, \tag{5}$$

$$\mathrm{MSE} = \frac{1}{n}\sum_{i=1}^{n}\left(X_i - Y_i\right)^2, \tag{6}$$

$$\mathrm{RMSE} = \sqrt{\frac{1}{n}\sum_{i=1}^{n}\left(X_i - Y_i\right)^2}. \tag{7}$$

The histogram of prediction errors provides further insight into the error distribution of the model. The correlation analysis provides valuable insight into the relationships between the variables in the dataset. A positive correlation indicates that as one variable increases, the other tends to increase as well, while

a negative correlation indicates the opposite. Weak or near-zero correlations suggest that the variables are independent of each other and do not share a significant linear relationship. For instance, as it is clear in Fig. 5, although there is a completely non-linear relationship between scale thickness with three other outputs, the proposed approach was able to predict all of them with a very low error showing the high capacity of utilizing the proposed metering system in related industries.

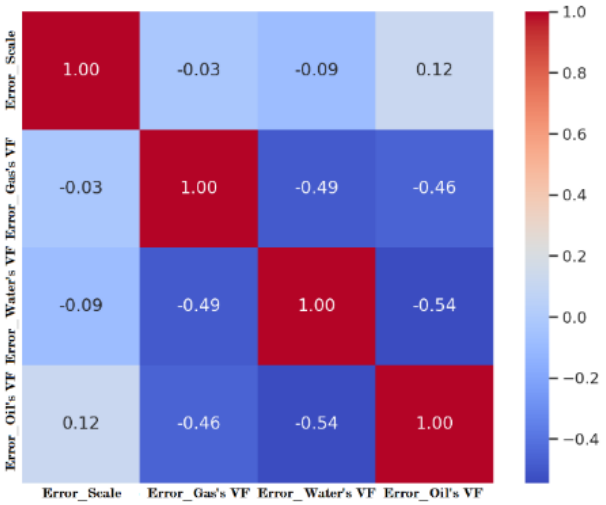

Fig. 5. Correlation and performance analysis of the proposed approach

To highlight the novelty and performance, the proposed metering system, its outcomes and main components are compared with that of some similar published papers in Table 1.

As demonstrated in Table 1, the proposed metering system uniquely combines simultaneous estimation of three-phase volume fractions and scale thickness with a minimal sensing configuration (one capacitance sensor, one gamma-ray source and one detector), thereby offering an improved balance between measurement capability, hardware simplicity and prediction accuracy as compared with existing approaches. In the comparison table, the proposed metering system has been compared with 7 similar and new published studies. The performance and accuracy of a gamma-ray attenuation sensor depend on the number of detectors and sources it uses. Adding more detectors and sources generally improves measurement accuracy. However, it also increases complexity, cost, power consumption and other challenges. Furthermore, using more gamma sources raises safety risks and regulatory issues, as handling radioactive materials is difficult. In this study, the sensor utilized was combined with a minimum number of detectors and sources to keep costs low and make it easier to manage. While this number of detectors and sources can be found in previous studies, the proposed approach possesses fewer MAE for all phases along with being able to measure scale thickness, too. While [3] reported just the VF of the water phase of a three-phases fluid, [17] and [18] just presented the prediction of scale thickness. Although they have reported fewer MAE for scale thickness, the current study has presented VFs beside scale thickness. Also, in [19], the authors have employed just one source detector and source, and then they reported the scale layer's thickness with an error of 0.46, which is about two times higher than that of the current study. The closest investigation in the comparison table is in [16], which has measured all volume fractions and scale thickness, simultaneously. While it has predicted scale thickness with an MAE of 0.029, being lower than the current approach, all of its reported VFs are higher than that of the proposed method. Reference [16] achieved an MAE of 0.321 for the gas phase, 1.977 for the water phase and 2.121 for the oil phase, respectively. These errors are about 12 times, 62 times and 64 times higher than that of the proposed metering system, correspondingly. More efficient network's structure, higher sensitivity of the capacitance-based sensor, and higher energy of the used gamma ray resulted in achieving the proposed metering system whose results highlight its novelty and great performance. The main novelty of this study is the simultaneous determination of three-phase volume fractions and scale layer thickness. In offshore oil fields, fluid proportions change continuously, which causes large measurement errors in traditional methods. While past studies usually focused on predicting either volume fractions or scale thickness separately, this work fills the gap by doing both at the same time. By combining simple, non-invasive

Table 1
Comparing some of three-phase-based published studies with the current study

Source	Gas's VF MAE	Water's VF MAE	Oil's VF MAE	Scale MAE	Source(s)	Detector(s)	Sensor(s)
[3]	0.318	1.531	1.614	–	1	1	Capacitance + Gamma-ray
[10]	3.68	0.33	3.75	–	1	1	Capacitance + Gamma-ray
[11]	1.6	0.29	1.67	–	1	1	Capacitance + Gamma-ray
[16]	0.321	1.977	2.121	0.029	1	2	Gamma-ray
[17]	–	–	–	0.01	1	3	Gamma-ray
[18]	–	–	–	0.07	2	2	Gamma-ray
[19]	–	–	–	0.46	1	1	Capacitance + Gamma-ray
Current study	0.027	0.032	0.033	0.24	1	1	Capacitance + Gamma-ray

sensors with an optimized ANN model, this approach provides a highly accurate and low-cost monitoring solution for industrial multiphase flows. In this study, the proposed method was successfully tested for a homogeneous flow regime in a laboratory setup, showing high accuracy. To expand this work in the future, the model can be updated to identify other flow regimes, such as stratified or annular flows. Also, future studies can evaluate the performance of this metering system under real industrial conditions with higher pressures and continuous flows. The superior performance of the proposed metering system originates from the integrated optimization of both the sensing hardware and the data-driven estimation model. Instead of relying on multiple radioactive sources or additional detectors to improve accuracy, this study combines a high-sensitivity twin rectangular fork-like capacitance sensor with a properly selected Co-60 gamma-ray source, allowing for complementary dielectric and density information to be extracted using only a single-source/single-detector configuration. The optimized MLP network effectively exploits these complementary measurements, resulting in simultaneous estimation of gas, water and oil volume fractions together with scale thickness while maintaining low hardware complexity and radiation exposure. Consequently, the proposed method provides an improved trade-off among accuracy, cost, implementation simplicity and operational safety as compared with existing approaches.

4. CONCLUSIONS

In this study, a novel, non-invasive metering system equipped with Artificial Intelligence (AI) has been proposed for the simultaneous and precise measurement of the volume fractions of oil, gas and water phases, as well as the scale layer thickness in pipelines. The proposed system utilized capacitance-based and gamma-ray attenuation sensors to collect data, which were then processed by an MLP ANN. Through rigorous simulations and theoretical models, data sets were generated using the COMSOL Multiphysics software and the Beer-Lambert law, respectively. ANN was trained and tested on these data, with performance evaluated across various configurations of network parameters. The results obtained from the MLP ANN indicate excellent accuracy, with MAE of 0.027, 0.32 and 0.033 for predicting the VFs of gas, water and oil phases, respectively. Additionally, scale layer thickness measurement yielded an MAE of 0.244. These results demonstrated that the proposed metering system can achieve high-precision measurements of multiple parameters in multi-phase flows, which are critical in many industrial applications. The integration of AI with sensor technologies not only enhanced the accuracy of measurement but also presented a promising solution for real-time, non-invasive monitoring of complex flow conditions. Overall, the proposed system represented a significant advancement in the field of multi-phase flow measurement, offering improved accuracy and versatility.

ACKNOWLEDGEMENTS

This research (Hala H. Alhashim) was funded/supported by the Deanship of Scientific Research, Imam Abdulrahman Bin Faisal University Dammam, Saudi Arabia Grant 2019-399-Sc.

Data Availability

The data generated and analyzed in this study are available from the corresponding author upon request.

REFERENCES

[1] G.S. Sestito, R. Álvarez-Briceño, G. Ribatski, M.M. da Silva, and L.P. de Oliveira, "Vibration-Based Multiphase-Flow Pattern Classification via Machine Learning Techniques," *Flow Meas. Instrum.*, vol. 89, p. 102290, 2023, doi: 10.1016/j.flowmeasinst.2022.102290.

[2] P. Mohindru, "Development of Liquid Level Measurement Technology: A Review," *Flow Meas. Instrum.*, vol. 89, p. 102295, 2023, doi: 10.1016/j.flowmeasinst.2022.102295.

[3] A.M. Mayet *et al.*, "Measuring Volume Fractions of a Three-Phase Flow without Separation Utilizing an Approach Based on Artificial Intelligence and Capacitive Sensors," *PLoS ONE*, vol. 19, no. 5, p. e0301437, 2024, doi: 10.1371/journal.pone.0301437.

[4] A. do Nascimento Wrasse, E.N. dos Santos, M.J. da Silva, H. Wu, and C. Tan, "Capacitive Sensors for Multiphase Flow Measurement: A Review," *IEEE Sensors J.*, vol. 22, no. 22, pp. 21391–21409, 2022, doi: 10.1109/JSEN.2022.3210467.

[5] Q. Marashdeh, B. Straiton, and P. Snyder, "Advanced Multi-Dimensional Capacitance Sensors Based Subsea Multiphase Mass Flow Meter to Measure and Monitor Offshore Enhanced Oil," *Tech4Imaging LLC*, Columbus, USA, 2024, doi: 10.2172/2335348.

[6] S. Thiele, M.J. da Silva, and U. Hampel, "Capacitance Planar Array Sensor for Fast Multiphase Flow Imaging," *IEEE Sensors J.*, vol. 9, no. 5, pp. 533–540, 2009, doi: 10.1109/JSEN.2009.2015008.

[7] L. Zarour, G.F. Malykhina, and Y.M. Hanafi, "Gamma-Ray Detection Simulation in Case of Non-Destructive Multiphase Oil Well Flow Measurement," in *Proc. Int. Conf. Cyber-Physical Systems and Control*, Cham, Switzerland: Springer, 2021, pp. 304–314, doi: 10.1007/978-3-031-20875-1_28.

[8] L. Chen, C. Xia, Z. Zhao, H. Fu, and Y. Chen, "AI-Driven Sensing Technology," *Sensors*, vol. 24, no. 10, p. 2958, 2024, doi: 10.3390/s24102958.

[9] A.M. Iliyasu, F. Fouladinia, A.S. Salama, G.H. Roshani, and K. Hirota, "Intelligent Measurement of Void Fractions in Homogeneous Regime of Two-Phase Flows Independent of the Liquid Phase Density Changes," *Fractal Fract.*, vol. 7, no. 2, p. 179, 2023, doi: 10.3390/fractalfract7020179.

[10] F. Fouladinia *et al.*, "A Novel Metering System Consisting of a Capacitance-Based Sensor, Gamma-Ray Sensor and ANN for Measuring Volume Fractions of Three-Phase Homogeneous Flows," *Nondestruct. Test. Eval.*, vol. 40, pp. 1–27, 2024, doi: 10.1080/10589759.2024.2375575.

[11] A.M. Mayet *et al.*, "Multiphase Flow's Volume Fractions Intelligent Measurement by a Compound Method Employing Cesium-137, Photon Attenuation Sensor, and Capacitance-Based Sensor," *Energies*, vol. 17, no. 14, p. 3519, 2024, doi: 10.3390/en17143519.

[12] M. Askari, A. Taheri, M. Mojtahedzadeh Larijani, A. Movafeghi, and H. Faripour, "A Gamma-Ray Tomography System to Determine Wax Deposition Distribution in Oil Pipelines," *Rev. Sci. Instrum.*, vol. 90, no. 7, p. 075103, 2019, doi: 10.1063/1.5095859.

[13] I. Stüwe, L. Zacherl, and C.U. Grosse, "Ultrasonic and Impact-Echo Testing for the Detection of Scaling in Geothermal Pipelines," *J. Nondestruct. Eval.*, vol. 42, no. 1, p. 18, 2023, doi: 10.1007/s10921-023-00926-0.

[14] J.P. Candeias, D.F. de Oliveira, M.J. dos Anjos, and R.T. Lopes, "Scale Analysis Using X-Ray Microfluorescence and Computed Radiography," *Radiat. Phys. Chem.*, vol. 95, pp. 408–411, 2014, doi: 10.1016/j.radphyschem.2013.03.007.

[15] R.S. de Freitas Dam, W.L. Salgado, R. Schirru, and C.M. Salgado, "Application of Deep Neural Network and Gamma-Ray Scattering in Eccentric Scale Calculation Regardless of the Fluids Volume Fraction Inside a Pipeline," *Appl. Radiat. Isot.*, vol. 188, p. 110353, 2022, doi: 10.1016/j.apradiso.2022.110353.

[16] R.S. de Freitas Dam, M.C. dos Santos, W.L. Salgado, B.L. da Cruz, R. Schirru, and C.M. Salgado, "Prediction of Fluids Volume Fraction and Barium Sulfate Scale in a Multiphase System Using Gamma Radiation and Deep Neural Network," *Appl. Radiat. Isot.*, vol. 201, p. 111021, 2023, doi: 10.1016/j.apradiso.2023.111021.

[17] C.M. Salgado, W.L. Salgado, R.S. de Freitas Dam, and C.C. Conti, "Calculation of Scales in Oil Pipeline Using Gamma-Ray Scattering and Artificial Intelligence," *Measurement*, vol. 179, p. 109455, 2021, doi: 10.1016/j.measurement.2021.109455.

[18] O. Taylan, M. Abusurrah, S. Amiri, E. Nazemi, E. Eftekhari-Zadeh, and G.H. Roshani, "Proposing an Intelligent Dual-Energy Radiation-Based System for Metering Scale Layer Thickness in Oil Pipelines Containing an Annular Regime of Three-Phase Flow," *Mathematics*, vol. 9, no. 19, p. 2391, 2021, doi: 10.3390/math9192391.

[19] A.M. Mayet *et al.*, "MLP ANN Equipped Approach to Measuring Scale Layer in Oil-Gas-Water Homogeneous Fluid by Capacitive and Photon Attenuation Sensors," *J. Nondestruct. Eval.*, vol. 44, no. 2, p. 35, 2025, doi: 10.1007/s10921-025-01193-8.

[20] S.M. Salehi, H. Karimi, A.A. Dastranj, and R. Moosavi, "Twin Rectangular Fork-Like Capacitance Sensor for Flow Regime Identification in Horizontal Co-Current Gas-Liquid Two-Phase Flow," *IEEE Sensors J.*, vol. 17, no. 15, pp. 4834–4842, Aug. 2017, doi: 10.1109/JSEN.2017.2708663.

[21] M.J. Berger *et al.*, "XCOM: Photon Cross Sections Database," NIST Standard Reference Database 8 (XGAM), National Institute of Standards and Technology, Gaithersburg, 2010, USA. [Online]. Available: https://www.nist.gov/pml/xcom-photon-cross-sections-database [Accessed: Feb. 24, 2025].

[22] L. Zhang and P.N. Suganthan, "A Survey of Randomized Algorithms for Training Neural Networks," *Inf. Sci.*, vol. 364-365, pp. 146–155, Sep. 2016, doi: 10.1016/j.ins.2016.01.039.

[23] K. He, X. Zhang, S. Ren, and J. Sun, "Deep Residual Learning for Image Recognition," in *Proc. IEEE Conf. Comput. Vis. Pattern Recognit. (CVPR)*, Las Vegas, NV, USA, Jun. 2016, pp. 770–778, doi: 10.1109/CVPR.2016.90.

[24] K. Levenberg, "A Method for the Solution of Certain Non-Linear Problems in Least Squares," *Q. Appl. Math.*, vol. 2, no. 2, pp. 164–168, 1944, doi: 10.1090/QAM/10666.

[25] D.W. Marquardt, "An Algorithm for Least-Squares Estimation of Nonlinear Parameters," *J. Soc. Ind. Appl. Math.*, vol. 11, no. 2, pp. 431–441, Jun. 1963.